Free energy and phase diagram of a triangular nonlinear lattice with a bistable substrate

1990 J. Phys. A: Math. Gen. 23 4553

(http://iopscience.iop.org/0305-4470/23/20/017)

J. Phys. A: Math. Gen. 23 (1990) 4553-4567. Printed in the UK

Free energy and phase diagram of a triangular nonlinear lattice with a bistable substrate

G Vlastou-Tsinganos†, N Flytzanis† and H Büttner‡

† Physics Department, University of Crete, Heraklion, Greece
‡ Physikalisches Institute, Universität Bayreuth, D-8580 Bayreuth, Federal Republic of Germany

Received 7 February 1990, in final form 21 June 1990

Abstract. A model consisting of atoms on a triangular lattice, with one degree of freedom, interacting with harmonic forces up to second neighbours and with a ϕ^4 on-site potential is studied. The system's free energy is calculated using an independent site approximation and a quantum variational 'ansatz'. Phase diagrams are constructed by minimizing the free energy, using the simulated annealing Monte Carlo method. They consist of 1D and 2D stable superstructures between which discommensurations intervene. The model is relevant to one degree of freedom systems as, e.g., free to rotate molecular groups.

1. Introduction

The competition between different ordering mechanisms in a system can result in a variety of phases which may range from commensurate, incommensurate, discommensurations and even spacially chaotic states. For example the anisotropic Ising model (ANNNI) (Elliot 1961) consists of a rather simple magnetic system, with competing nearest and next-nearest neighbour interactions, which can reproduce many of the features encountered in real magnetic systems. Its phase diagram is very rich, presenting modulated structures (Selke 1988, Bak and von Boehm 1980), but its applicability to real non-magnetic systems, involving continuous lattice displacements, is limited due to the definite values spins can take. In lattice models a double well on-site potential with nearest and next-nearest neighbour interactions, despite its simplicity, allows both continuous displacements and bistable behaviour, so that it can describe a large variety of physical systems. The equivalence of this model to an Ising one with infinite range interactions, for one-dimensional systems has been proved by Axel and Aubry (1981). The physical origin of the ϕ^4 nonlinear potential used can be attributed to either the substrate material, as in noble gas monolayers (Gordon and Villain 1985), or the sterical hindrance potential of NO_2 groups in $NaNO_2$ (Heine and McConnell 1984), or to the ion and its electronic shell nonlinear interaction in perovskites (Bilz *et al* 1987), or to a molecular group free to rotate, as in biphenyl (Benkert *et al* 1987) and $LiIO_3$ (Coquet *et al* 1988). Furthermore it is of great importance to know the commensurate structures for a given model in order to describe various structural phase transitions into these states; one of the important transitions is the incommensurate-commensurate transition found in many crystals (see the various articles in vol II of Blinc and Levanyuk 1986). An important example is K_2SeO_4 which was studied theoretically some time ago (Bilz *et al* 1982). There it was shown that the low temperature state with period 3 is a stable solution within the nonlinear model.

0305-4470/90/204553+15$03.50

Although the ϕ^4 potential is sometimes approximated by a double quadratic one in order to facilitate analytical computations (Büttner and Heym 1987, Vlastou *et al* 1990), we study the problem here without these approximations. In a one-dimensional model with a single well ϕ^4 potential a number of commensurate phases were described by Frosch and Büttner (1985). We are here extending this work to a two-dimensional triangular lattice with a double well on-site ϕ^4 potential and first-second neighbour interactions. A quantum mechanical variational treatment is used to derive analytically the free energy. The numerical evaluation uses the simulated annealing Monte Carlo method, in order to construct the phase diagram of the system, which turns out to consist of a great variety of structures, commensurate or incommensurate. This multiplicity in phases is attributed to competing mechanisms. The on-site potential tends to lock the atoms on the lattice sites, and the neighbouring interactions favour arbitrary configurations. The effect of temperature is also crucial here, because the interaction parameters are temperature dependent and thermal fluctuations act antagonistically to the ordering mechanisms.

In section 2 we calculate the free energy of our model using a variational 'ansatz' and reduce the equations that will give us the temperature dependence of the variational parameters. In section 3 we use the simulated annealing Monte Carlo method (SAMC), to minimize the free energy and construct the phase diagrams. In the last section we summarize and discuss the results for the phase diagrams.

2. Free energy evaluation

The Hamiltonian of our two-dimensional triangular lattice model for the atomic displacement $u_{n,m}$, normal to the surface, is:

$$H=\frac{1}{2}\sum_{n,m}\left(-\frac{\hbar^2}{M}\frac{\partial^2}{\partial u_{n,m}^2}+f_1[(u_{n+1,m}-u_{n,m})^2+(u_{n,m+1}-u_{n,m})^2+(u_{n-1,m+1}-u_{n,m})^2]\right.$$
$$\left.+f_2[(u_{n+1,m-2}-u_{n,m})^2+(u_{n+2,m-1}-u_{n,m})^2+(u_{n+1,m+1}-u_{n,m})^2]\right)$$
$$+\sum_{n,m}\left[\frac{1}{4}g_4\left(u_{n,m}^2-\frac{g_0}{g_4}\right)^2\right]. \tag{1}$$

The first term is the kinetic energy operator of the atoms with mass M. The second and third terms are the potential energies for the harmonic nearest-(f_1) and next-nearest-(f_2) neighbour interactions (figure 2(b) below). The last term is a double well on-site unharmonic ϕ^4 potential ($g_0, g_4>0$). The true independent parameters of our Hamiltonian are $c_1=f_1/2g_0$ and $c_2=f_2/2g_0$, if displacements are measured in units of $\sqrt{g_0/g_4}$ and energies in units of g_0^2/g_4.

Since we are interested in determining the ground-state structures for finite temperatures, we have to evaluate the free energy F of the system, which is not an easy task. Exact quantum mechanical calculation of the free energy has not been done for a nonlinear lattice, except for some completely integrable one-dimensional systems using the Bethe ansatz (Toda 1981). We are therefore forced to use an approximation, which is the independent-site appoximation improved by choosing different variational parameters at each site, for both the local oscillator frequency $\omega_{n,m}$ and the displacement $\alpha_{n,m}$ of the oscillator. The idea is to approximate the true free energy F, from above, to first order, by the free energy of a known system F_0 plus a correction term (Feynman

1974),

$$F \leqslant \tilde{F} = F_0 + \langle H - H_0 \rangle_0. \tag{2}$$

This is usually referred to as the 'minimum principle', since it sets an upper bound to F. The Hamiltonian H_0, which is used for comparison with H, is that of a set of independent displaced harmonic oscillators:

$$H_0 = \frac{1}{2} \sum_{n,m} \left[-\frac{\hbar^2}{M} \frac{\partial^2}{\partial u_{n,m}^2} + \omega_{n,m}^2 (u_{n,m} - \alpha_{n,m})^2 \right]. \tag{3}$$

It has been shown by Feynman and Kleinert (1986) that the true value of the free energy is almost identical to $\tilde{F}$ at high temperatures and differs from it a few percent as temperature lowers. A further improvement of the method is the choice of more elaborated trial functions H_0 so that the second term in (2) vanishes (Giachetti *et al* 1988).

The expectation value in equation (2) noted as $\langle \ldots \rangle_0$ is calculated with the known harmonic density matrix of H_0:

$$\rho_0(y, y) = \sqrt{\frac{\omega}{2\pi \sinh(\omega/\tau)}}\, e^{-\omega \tanh(\omega/2\tau) y^2} \tag{4}$$

where we have set for simplicity $\hbar = M = 1$ and $\tau = k_B T/\hbar$. After simple but lengthy calculations we arrive at the free energy expression as a function of $\alpha_{n,m}$ and $\omega_{n,m}$

$$\begin{aligned} 2\tilde{F} = \sum_{n,m} \Bigg\{ & \omega_{n,m} + 2\tau \ln(1 - e^{-(\omega_{n,m}/\tau)}) - \frac{\omega_{n,m}^2}{2\gamma_{n,m}} + \sum_{\langle NN \rangle} \frac{1}{2} c_1 \left[(\alpha_{\langle NN \rangle} - \alpha_{n,m})^2 + \frac{1}{2\gamma_{\langle NN \rangle}} \right] \\ & + \sum_{\langle NNN \rangle} \frac{1}{2} c_2 \left[(\alpha_{\langle NNN \rangle} - \alpha_{n,m})^2 + \frac{1}{2\gamma_{\langle NNN \rangle}} \right] \\ & + \frac{1}{2\gamma_{n,m}} \left[3(c_1 + c_2) + g_0 + 3g_4 \alpha_{n,m}^2 + \frac{3g_4}{4\gamma_{n,m}} \right] \\ & + g_0 \alpha_{n,m}^2 + \frac{1}{2} g_4 \alpha_{n,m}^4 + \frac{g_0^2}{2g_4} \Bigg\} \end{aligned} \tag{5}$$

where $\langle NN \rangle$ and $\langle NNN \rangle$ denote summation over first and second neighbours to the (n, m) atom respectively, while we define:

$$\gamma_{n,m} = \omega_{n,m} \tanh\left(\frac{\omega_{n,m}}{2\tau} \right). \tag{6}$$

The variational parameters are then determined by an extremal condition at each site: $\partial\tilde{F}/\partial\alpha_{n,m} = 0$, $\partial\tilde{F}/\partial\omega_{n,m} = 0$ and they are as follows:

$$\frac{\partial \tilde{F}}{\partial \alpha_{n,m}} = \sum_{\langle NN \rangle} c_1 (\alpha_{\langle NN \rangle} - \alpha_{n,m}) + \sum_{\langle NNN \rangle} c_2 (\alpha_{\langle NNN \rangle} - \alpha_{n,m}) + g_0 \alpha_{n,m} + g_4 \alpha_{n,m}^3 + \frac{3g_4 \alpha_{n,m}}{2\gamma_{n,m}} \tag{7}$$

$$\frac{\partial \tilde{F}}{\partial \omega_{n,m}} = \frac{1}{2} \left[3(c_1 + c_2) + \frac{1}{2} \left(g_0 - \omega_{n,m}^2 + 3g_4 \alpha_{n,m}^2 + \frac{3g_4}{2\gamma_{n,m}} \right) \right] \frac{\partial}{\partial \omega_{n,m}} \left(\frac{1}{\gamma_{n,m}} \right). \tag{8}$$

These equations are a coupled nonlinear discrete system, where the first one contains

a fourth-order recurrence relation for $\alpha_{n,m}$ but the second one can easily be solved for $\alpha^2_{n,m}(\omega_{n,m})$. For those low periodicities, for which the different average atomic positions are not more than two, the above equations can be reduced to a rather simple system of nonlinear equations. In the appendix we give the respective equations for some simple structures: para-electric, 1×1, 2×1, 3×1 symmetric and 4×1.

Solving the above nonlinear equations we can determine the periodic structure with the lowest free energy. This allows us to construct a phase diagram in the three-parameter space (c_1, c_2 and temperature τ), or more conveniently in the two-parameter (c_1 and τ) space by keeping c_2 constant. The numerical solution though of the equations is only practical for the above mentioned low periodicities. For higher periodicities, however, of the type $N\times1$ (for $N>4$) or $N\times M$ (for N, $M\geq2$), an alternative approach is to directly minimize the free energy using the powerful simulated annealing Monte Carlo method (SAMC) (Kirkpatrick *et al* 1983). This method has the advantage of locating the global minimum of a multivariable function. The method involves a search over the configuration space with a specific procedure that ensures the possibility to escape from local minima in the search for the global minimum. The success of this search depends strongly on the procedure and the criteria are described elsewhere (Vlastou *et al* 1990).

Our phase diagrams are thus constructed by scanning the (c_1, c_2, τ) space by the SAMC method and finding at each point the periodic structure that corresponds to the global minimum. One-dimensional structures were checked, using different initial conditions and search patterns for different SAMC parameters, up to period 15×1 and two-dimensional up to 3×3. At very low temperatures there are many competing structures which lie close in configuration space and are separated by large barriers. Thus SAMC search patterns must be adjusted to avoid convergence problems (e.g. increase the initial fictitious temperature and reduce the displacement step). Where possible, diagram points were double checked by the direct numerical solution of the set of nonlinear equations for the known structures. Results obtained by both methods are identical.

3. The phase diagrams

Since both force constants c_1 and c_2 are independent parameters in our model, the (c_1, τ) phase diagrams were made for the three representative values of c_2: 0.2, −0.2, −0.5 in order to reveal a complete picture of the effect of temperature on the lattice.

(a) $c_2=0.2$. Figure 1 presents the phase diagram for $c_2=0.2$, which appears rather simple containing only three periodic structures. The period 1×1 and symmetric 3×3 (also given as $\sqrt{3}\times\sqrt{3}$ shown in figure 2(*a*)) structures are expected here since they dominate the $\tau=0$ classical diagram presented in (Vlastou *et al* 1990) (figure 2) for the respective c_1 and c_2 values. What is new here is the existence of the so-called para-electric phase, which is characterized by an average displacement zero ($\alpha=0$) for each atom. This phase is found to be the ground state for high temperatures, since the kinetic energy provided by the temperature raises the atoms above the potential barrier, visiting both wells, with their average position at $\alpha=0$. When c_1 is negative enough, structures with opposite average displacements for nearest neighbours become antagonistic, and as a result of this, the $\sqrt{3}\times\sqrt{3}$ structure in figure 1 remains ground state for high temperatures. Using a simple mean-field approximation (Janssen and Tjon 1982) we can show that effectively the force constants c_1 and c_2 increase with

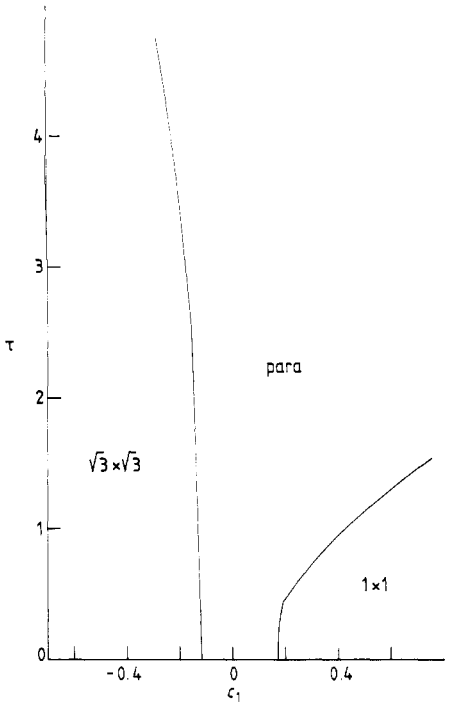

Figure 1. Phase diagram in the τ, c_1 plane for $c_2 = 0.2$.

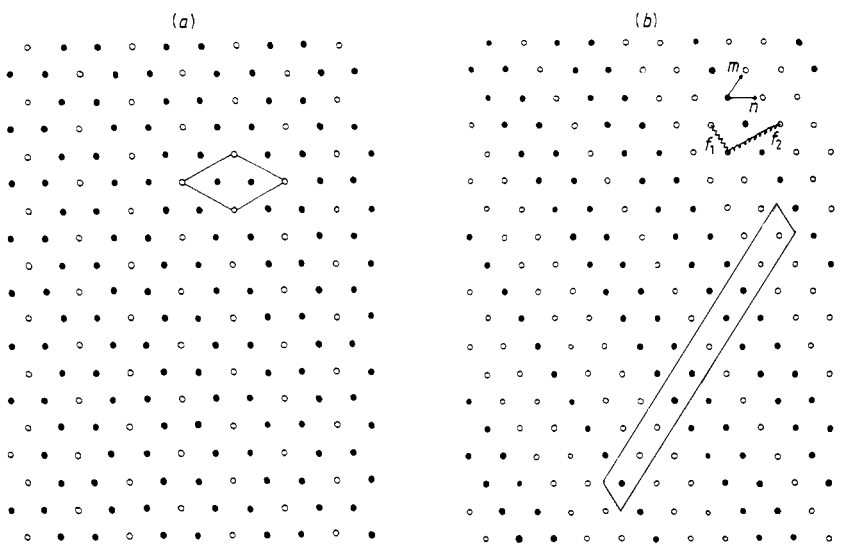

Figure 2. (*a*) The $\sqrt{3} \times \sqrt{3}$ structure with its unit cell. (*b*) The 10×1 1D structure.

increasing temperature. Indeed, the atoms move towards the centre of the potential barrier as c_1 or temperature increases.

Our calculation of the free energy has included quantum effects as for example the zero point motion at $\tau = 0$. Therefore we expect a discrepancy between the classically obtained $\tau = 0$ phase diagram presented in Vlastou *et al* (1990) paper, and the corresponding results presented here. Actually, the point $c_1 = 0$, $\tau = 0$ in figure 1 does not separate the two phases 1×1 and $\sqrt{3} \times \sqrt{3}$ as was found in the classical case. There is a gap between the two phases occupied by the $\alpha = 0$ phase even as low temperatures as $\tau \to 0$, which means that the effective potential has only one minimum at $\alpha = 0$.

(b) $c_2 = -0.2$. For this choice of c_2 the phase diagram shown in figure 3 displays the great variety of phases that can appear there. Starting from negative c_1 values we note how the 2×1 structure persists for very high temperatures despite the strong thermal fluctuations. This is achieved by the strong and opposite neighbouring displacements that keep the atoms, on the average, the furthest apart. The symmetric 3×1 $(+0-)$ phase appears over certain temperatures where 3×3 (asymmetric) and 3×1 $(++-)$ no longer are ground states. It is astonishing to see the regular succession of superstructures, for $c_1 > 0$, starting from 3×1 up to 8×1, for very low temperatures. The respective region in the classical $\tau = 0$ diagram was difficult to reveal clearly because the energy minima were close by. The configurations of these periodicities (1D structures for $4 \leqslant N \leqslant 8$) are: for N even $N/2$ successive positive mean displacements and $N/2$ negative ones. For N odd: $(N-1)/2$ successive positive followed by $(N+1)/2$ negative ones. As a result of this the coordination numbers n_1 and n_2 defined as the average number of opposite neighbours (first and second) per site, are $n_1 = 4/N$ and $n_2 = 8/N$. Configurations of higher periodicity $(N > 8)$ were found for higher temperatures $(\tau > 0.2)$ and in the border lines between the superstructures. They are usually described (Janssen 1986) as a series of integers indicating the number of consecutive particles with the same sign of the solution. For example, the structure 10×1 (shown in figure 2(*b*)) with signs of displacements as $(++--+--++-)$ will be indicated as $(2^2 1)^2$. The configurations of all these periodic structures appearing for

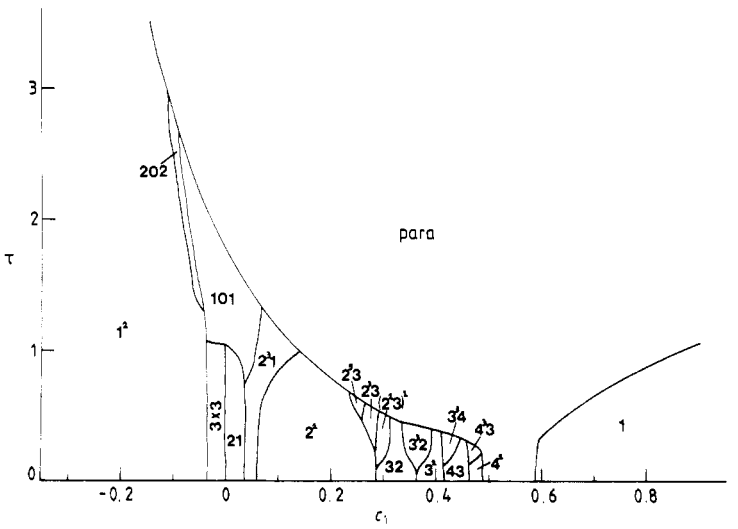

Figure 3. Phase diagram in the τ, c_1 plane for $c_2 = -0.2$. Structures' notation is explained in the text.

$c_1 > 0.2$, are such that $n_2 = 2n_1$, due to the fact that no less than two consecutive particles have the same sign for the displacement. An exception is the 7×1 structure found between 3×1 and 4×1, for which $n_1 = \frac{8}{7}$, $n_2 = 2$. For a discussion of similar structures in ANNNI-like models see the current state of the art review by Selke (1988), where the complicated issue of the appearance of commensurate and incommensurate states is discussed.

The para-electric phase is unstable classically at absolute zero and therefore it never appeared in the $\tau = 0$ classical diagram. Here, there is a small interval for $0.50 < c_1 < 0.58$ at very low temperatures, where the para-phase is ground state. 1×1 then follows for $c_1 > 0.58$ and evolves to the $\alpha = 0$ state with increasing temperature. Strong first neighbouring attraction seems to favour the 1×1 configuration as ground state, up to high temperatures.

Direct solutions of our system of nonlinear equations provide us with the three graphs presented in figure 4 where the variational parameters α and ω as well as the free energy are plotted against $c_1 + c_2$ for the structures 2×1, 1×1 and $\alpha = 0$. What is evident here is that: (*a*) the 2×1 structure exists as a solution of the respective equations and is stable (as will be explained later), only up to $c_1 + c_2 = -0.1$ for $\tau = 0.2$ which is in agreement with its being ground state well below this limit; (*b*) the 1×1 state does not exist as a stable structure below $c_1 + c_2 = 0.38$ at $\tau = 0.2$ and has actually a lower free energy than the $\alpha = 0$ phase for $c_1 + c_2 > 0.38$. This is in good agreement with the phase diagram of figures 1 and 3 but also makes a prediction about our next phase diagram of figure 6 for $c_2 = -0.5$, that 1×1 will appear as ground state (compared with $\alpha = 0$) at $c_1 > 0.88$. (*c*) While the mean atomic displacements for 1×1 emerge from zero and increase with $c_1 + c_2$, the respective α for the 2×1 structure never becomes zero due to the repulsive interaction that prevents the atoms to move towards the centre of the double well. This is the physical reason behind the existence of a 5×1 (202) structure, with an atomic mean displacement very close to zero, in the border of 2×1 with 3×1 symmetric (101) or the para-phase.

The diagrams presented in figure 5 show us the explicit dependence of our parameters α, ω and the free energy, on the temperature for the 1×1 and 2×1 structures. The high temperature limit is more conveniently displayed by plotting $1/\tau$ instead of τ.

(c) $c_2 = -0.5$. Our last phase diagram of τ against c_1 for fixed $c_2 = -0.5$ is presented in figure 6. The superstructures found here extend up to period 15, while the discommensurations intervene them. In order to better describe and give some insight to the occurrence of the periodic structures, we introduce the wavevector $q = 2\pi s/N$ for a modulation α_n (index m is omitted since we are concerned only with 1D structures in this part of the diagram and lattice spacing is taken as 1) (Janssen 1986). The number $2s$ is the number of sign changes within one period consisting of N atoms. A solution though is not uniquely determined by its wavevector q or $q_0 = s/N$ (half the number of sign changes per atom).

It has been very useful to plot the average number of opposite sign neighbours n_1 and n_2 for the $1-d$ structures of the triangular lattice, against the number s/N, as shown in figure 7. All the periodic structures, irrespectively of their configuration, seem to have their coordination number n_1 lying on a straight line with slope 4. The second neighbour coordination number n_2 for all the structures seems to cover all the space (for $N \to \infty$) between the n_1 line, the limiting n_2 line with slope 8 and the line $n_2 = 2$. Let us remark on certain points which are of interest in this diagram. (*a*) The period 1 structure and the para-phase are at the origin of figure 7. (*b*) 2 is the maximum

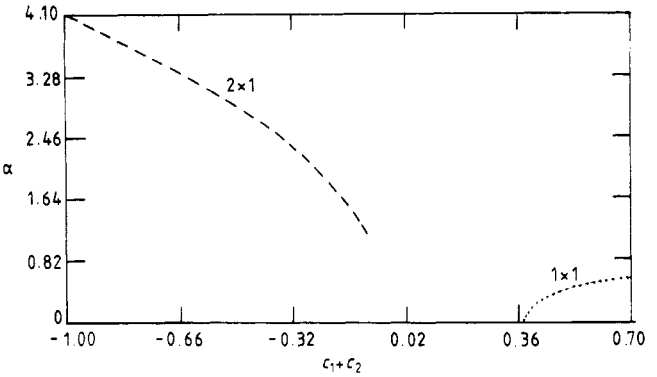

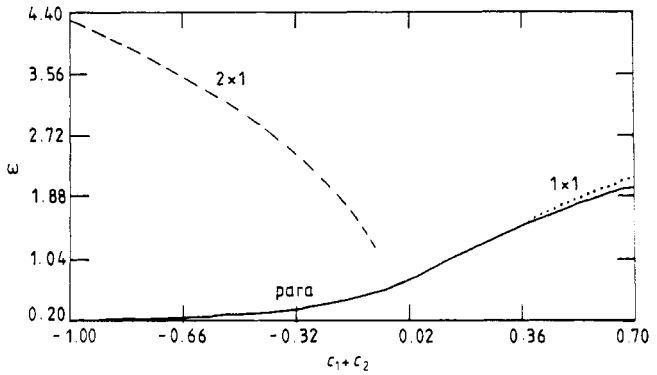

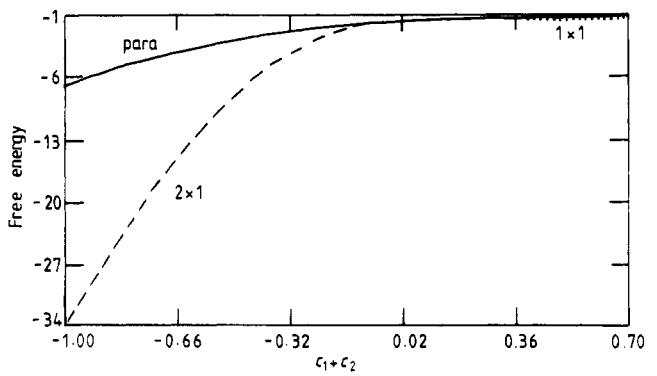

Figure 4. Plot of α, ω and F as functions of $c_1 + c_2$ for para, 1×1 and 2×1 at $\tau = 0.2$.

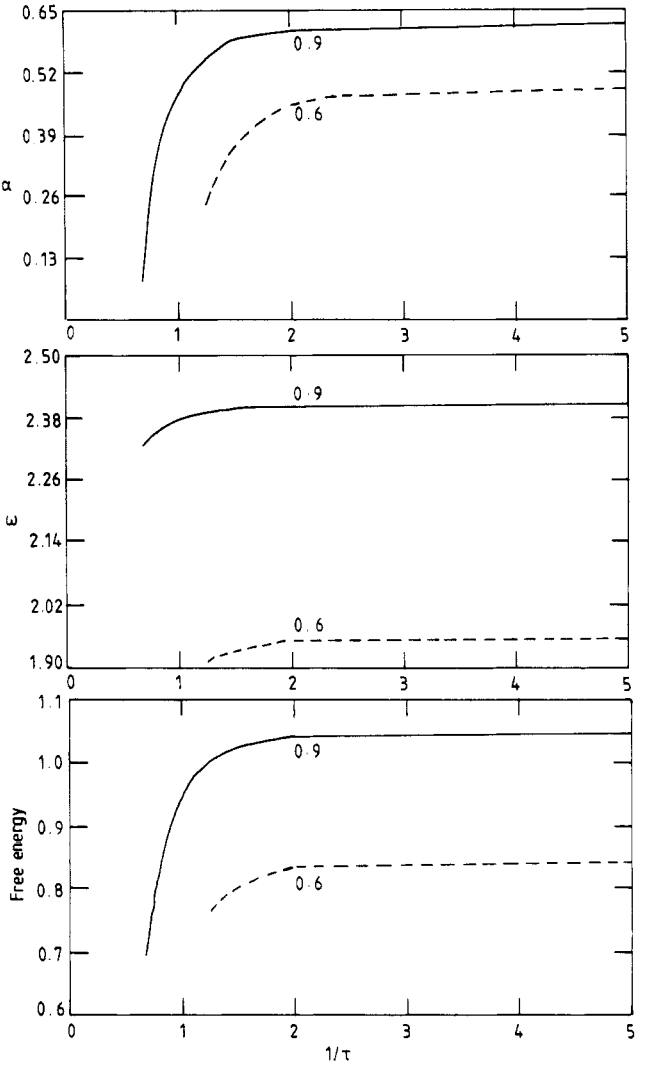

Figure 5. Plot of α, ω and F as functions of $1/\tau$ for $c_1 + c_2 = 0.6, 0.9$ for the 1×1 periodicity.

number of average opposite sign neighbours one atom can have. (*c*) n_1 is always less than n_2 and the maximum value n_2 can take is $2n_1$. (*d*) $n_2 = 2n_1$ can occur only to structures of $s/N \leqslant \frac{1}{4}$. (*e*) Structures with the same s/N number may or may not have the same n_2.

The basic features of the dependence of n_1 and n_2 on s/N are closely related to the phase diagrams of our model. Let us take for example the sequence of periodic structures close to the curve, which is the limit of the para-phase for $c_1 > 0$. The structures found as ground states with increasing $c_1 > 0$ lie exactly on the lines $n_1 = 4(s/N)$ and $n_2 = 8(s/N)$ for $s/N \leqslant \frac{1}{4}$. The ratios s/N can be generated as rational numbers between two fractions in the following way. Start with i/j and k/l and produce $(i+k)/(j+l)$ and $(i+2k)/(j+2l)$ and $(2i+k)/(2j+l)$ and iterate this procedure infinitely many times (Axel and Aubry 1981). Similarly, the structures found for $0 < c_1 < 0.4$ are those in the graph of figure 7 with $n_2 = 2$ and for $\frac{1}{4} \leqslant s/N \leqslant \frac{1}{3}$.

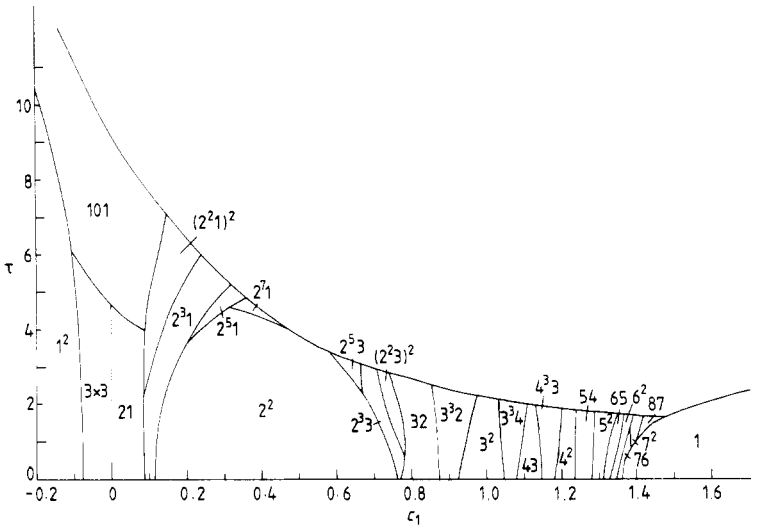

Figure 6. Phase diagram in the τ, c_1 plane for $c_2 = -0.5$.

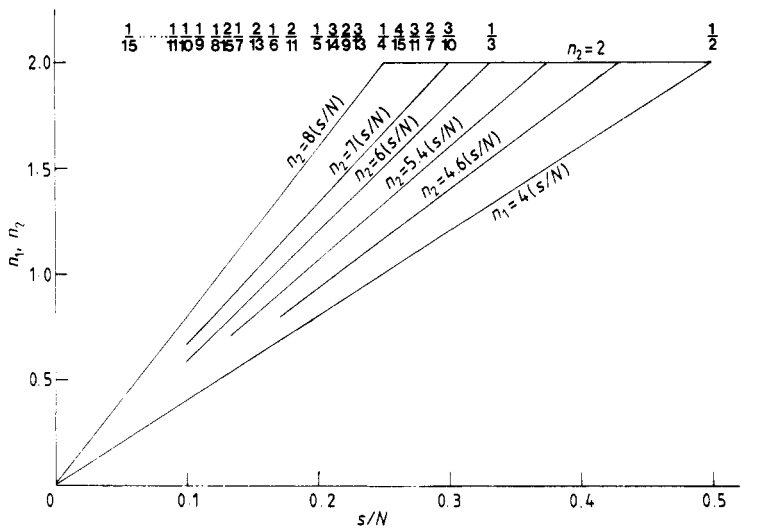

Figure 7. Plot of the 'coordination' numbers n_1 and n_2 against s/N for the triangular lattice. The fractions on the top of the diagram indicate the s/N of the structures found in our phase diagrams and whose n_1 and n_2 follow the enclosing triangle.

The physical reason behind the occurrence of those specific periodic structures in our phase diagram (among hundreds), whose n_2 numbers follow the limiting lines $n_2 = 8(s/N)$ and $n_2 = 2$, is that since they occur for increasing $c_1 > 0$ values they must have the minimum n_1 value and the maximum n_2 value in order to reduce their free energy. Also a prediction can be made, considering the specific configurations of those structures, if we are to further investigate our phase diagrams for higher periodicities and finer c_1 grid.

4. Concluding remarks

Using a variational principle we derive simple analytic expressions for the free energy of a one-component coupled atomic system with a bistable substrate. The thermal averages can be done analytically for a large class of bistable substrates, but we only considered the ϕ^4 case, because it is simple and there exist calculations to compare with 1D. For a more general substrate, if it is also steep for large displacements, we do not expect qualitative differences. This does not include the cos u term as in the 2D version of the Frenkel-Kontorova model [Vlastou *et al* 1990]. The variational principle used, is better than mean field since it uses both static and dynamic quantities as variational parameters, i.e. the average position and the local oscillation frequency of a set of effective oscillators, which to first approximation can be considered independent, but variationally connected. The variational parameters are determined by direct minimization of the free energy, using the simulated annealing Monte Carlo method, which has proved very efficient to find the global minimum subject to the boundary conditions only, i.e. finite size.

We have determined the ground states for a range of temperatures which appear in the phase diagrams as a series of periodic structures consisting of commensurate (superstructures) in one- and two-dimensions and discommensurations in 1D. The different parameters of our model may correspond to different materials or varying pressure. Discommensurations occur as an intermediate phase between two superstructures. They are characterized by a piecewise nearly constant phase function and they can be seen as the nucleus for the formation of a domain wall related to the periodic structure it contains. All the structures found are 1D except the $\sqrt{3}\times\sqrt{3}$, and a 3×3 structure, even though other 2D structures were searched for. This result is in agreement with previous work on the corresponding classical model at $\tau=0$ (Vlastou *et al* 1990). In a triangular Ising model in a field with nearest- and second-nearest-neighbour interactions (Kaburagi *et al* 1974), the only other structure was 2×2 between the $\sqrt{3}\times\sqrt{3}$ and the 3×1 structures. For the range of parameter values considered it was never the ground state in our case. In a study of the classical Heisenberg and planar model (XY) (Katsura *et al* 1986), a weak constraint condition wasused in the Fourier components of the spin length instead of the unit length spin. This allowed an analytic solution for the problem and then of course it was verified that the ground states satisfied on top the strong constraints. There again no 2D structures, except the $\sqrt{3}\times\sqrt{3}$, were found.

We have also investigated large complicated structures consisting of 3×3 domains, separated by domain walls whose core is 2×2. They were found to be stable but never the ground state. We have no definite answer why there are no more 2D structures, except to point out the higher degree of frustration that one has to cope with in 2D structures. By considering also the n_1 and n_2 numbers one can easily conclude that in the region where $\sqrt{3}\times\sqrt{3}$ is the ground state, it is unlikely that any other 2D similar structure has lower energy. Of course one must take also into account configurational entropy, which should be larger for the 2D patterns, so that they could become important at high temperatures, and that is the reason we looked at the large size patterns. It is also possible that the lattice symmetry plays a role, and in fact for an inhomogeneous model more complicated structures could appear. This question is under inevestigation.

Just below the critical temperature (above which the para-phase is ground state) in the phase diagram shown in figure 6, there are infinitely many phases in the limit $N\to\infty$. So, if one increases the resolution of the parameter c_1, one finds that the

interval over which a structure with a given wavevector of s/N is the ground state, becomes narrower and one can find always a value of c_1 for which a given wavevector is the wavevector of the ground state. Therefore the line is practically covered by periodic structures whose s/N numbers (or wavevectors) are rational and spaced infinitely close to one another. An irrational number could be approximated by a nearby rational corresponding to large N, and the corresponding structure should be looked for near the disorder limit, where the structures become dense in the interaction parameter space. In our case with maximum $N = 15$ we cannot describe well the structure near an incommensurate one. Our model though, satisfies the conditions set by (Janssen 1986), in order to have an incommensurate phase: (*a*) there is interaction at least up to second neighbours; (*b*) there is competition (c_1, c_2) and (*c*) there is a nonlinear interaction (ϕ^4) for the stabilization, which is in competition with interparticle forces. In figure 8 a plot is presented of the wavevector q or s/N against c_1 (it could also be another parameter of the model) for $\tau = 0.5$ and $c_2 = -0.5$. Periodicities up to 30×1 were examined over a range of c_1 values. The diagram clearly reveals a part of a '*devil's staircase*', which seems to continue for larger values of c_1. Whether the '*devil's staircase*' at this temperature is complete or incomplete cannot be determined from our calculations since it is very difficult to find.

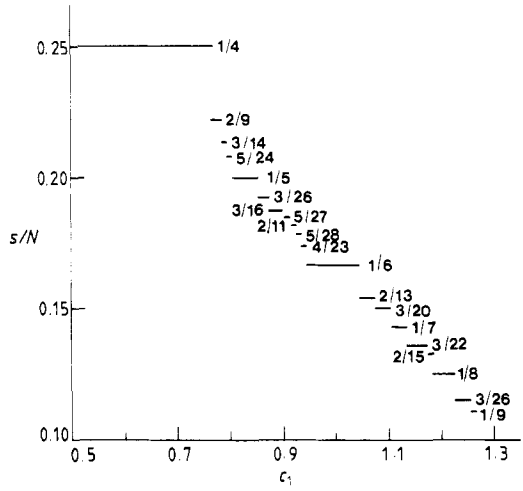

Figure 8. Plot of s/N against c_1 showing a '*devil's staircase*' for $c_2 = -0.5$ at $\tau = 0.5$.

Our method cannot determine incommensurate structures. Even the discrete mapping method (in 1D) (Jensen *et al* 1984), is plagued by numerical errors. One way used in the literature to decide, therefore, whether your system accepts incommensurate structures is to look for a '*devil's staircase*' and determine whether it is complete or incomplete. In our case with maximum $N = 30$ and low $\tau = 0.5$ the existence of an incommensurate state cannot be concluded. It is known from other models, however, that there exists a finite temperature where incommensurate states first appear, but it is usually very elaborate to find this temperature even in the mean field (Selke 1988).

The free energy calculations can be improved at low temperatures, as was done in Gianchetti *et al* (1988), by the introduction of an effective potential. This will include the smearing out of the nonlinear potential due to the quantum fluctuations. This

correction is not important at high temperatures and at any temperature for narrow potentials (high ω).

The linear stability of the structures found is not possible to be directly checked. The SAMC method used though, due to its random sampling alogorithm, provides us with structures that are stable against small oscillations. The positiveness of the effective oscillator strength $\omega_{n,m}$ is a sufficient but not necessary condition for stability. It is certain of course that the structures found as ground states have $\omega_{n,m} > 0$.

One example of a magnetic system where several commensurate phases have been observed is CeSb (Fisher *et al* 1978). In a temperature range from 16.1-2.2 K, six structures were found, by neutron diffraction, their s/N numbers being (with reducing temperature) $\frac{1}{3}$, $\frac{4}{13}$, $\frac{2}{7}$, $\frac{5}{18}$, $\frac{3}{11}$ and $\frac{1}{4}$, (containing several zero displacements). If we follow a line in figure 7 connecting ($c_1 = 0$, $\tau = 7.5$) and ($c_1 = 0.7$, $\tau = 1.5$) we go through the following sequence of structures: $\frac{1}{3}$, $\frac{3}{10}$, $\frac{2}{7}$, $\frac{3}{11}$, $\frac{1}{4}$. Rare earth compounds have been found, whose phase diagrams exhibit a '*devil's staircase*' part, that may correspond to an incommensurate phase or even a chaotic regime (Bak 1982). The existence, however of chaotic states has been questioned by Aubry (1983), due to the inaccuracies in the numerical solution of the mapping method (if a large number of iterations is involved) since the chaotic states correspond to positive Liapunov exponents. They should not be expected to be ground states since they correspond to unstable situations.

The natural next step in extending our model is to consider atoms having two degrees of freedom. This can be relevant in explaining the β-phase of $LiIO_3$ and give a better insight into the incommensurate phase of biphenyl, which has been so far considered as a one degree of freedom system (Benkert *et al* 1987).

Appendix

In the following we present the equations for the free energy (per site) and its variational equations for $\alpha_{n,m}$ and $\omega_{n,m}$ in the cases of $\alpha = 0$, 1×1, 2×1 and 4×1 periodicities.

(*a*) Para-phase, $a_{n,m} = 0$:

$$2\tilde{F} = \omega + 2\tau \ln(1 - e^{-(\omega_{n,m}/\tau)}) + \frac{g_0^2}{2g_4} + \frac{1}{2\gamma}\left[6(c_1 + c_2) + g_0 - \omega^2 + \frac{3g_4}{4\gamma}\right] \tag{A1}$$

$$\frac{\partial \tilde{F}}{\partial \omega} = \frac{1}{2}\left\{3(c_1 + c_2) + \frac{1}{2}\left[g_0 - \omega^2 + \frac{3g_4}{2\gamma}\right]\right\}\frac{\partial}{\partial \omega}\left(\frac{1}{\gamma}\right) = 0. \tag{A2}$$

(*b*) Period 1:

$$2\tilde{F} = \omega + 2\tau \ln(1 - e^{-(\omega_{n,m})/\tau})) + g_0\alpha^2 + \frac{1}{2}g_4\alpha^4 + \frac{g_0^2}{2g_4} + \frac{1}{2\gamma}\left[6(c_1 + c_2) + g_0 + 3g_4\alpha^2 + \frac{3g_4}{4\gamma} - \omega^2\right] \tag{A3}$$

$$\frac{\partial \tilde{F}}{\partial \alpha} = g_0\alpha + g_4\alpha^3 + \frac{3g_4\alpha}{2\gamma} = 0 \tag{A4}$$

$$\frac{\partial \tilde{F}}{\partial \omega} = \frac{1}{2}\left\{3(c_1 + c_2) + \frac{1}{2}\left[g_0 + 3g_4\alpha^2 + \frac{3g_4}{2\gamma} - \omega^2\right]\right\}\frac{\partial}{\partial \omega}\left(\frac{1}{\gamma}\right) = 0. \tag{A5}$$

(*c*) Period 2(+−):

$$2\tilde{F} = \omega + 2\tau \ln(1 - e^{-(\omega_{n,m}/\tau)}) + g_0\alpha^2 + \frac{1}{2} g_4\alpha^4 + \frac{g_0^2}{2g_4} + 8(c_1 + c_2)\alpha^2 + \frac{1}{2\gamma}\left[6(c_1 + c_2) + g_0 + 3g_4\alpha^2 + \frac{3g_4}{4\gamma} - \omega^2\right] \tag{A6}$$

$$\frac{\partial\tilde{F}}{\partial\alpha} = 8(c_1 + c_2)\alpha + g_0\alpha + g_4\alpha^3 + \frac{3g_4\alpha}{2\gamma} = 0 \tag{A7}$$

$$\frac{\partial\tilde{F}}{\partial\omega} = \frac{1}{2}\left\{3(c_1 + c_2) + \frac{1}{2}\left[g_0 + 3g_4\alpha^2 + \frac{3g_4}{2\gamma} - \omega^2\right]\right\}\frac{\partial}{\partial\omega}\left(\frac{1}{\gamma}\right) = 0. \tag{A8}$$

(*d*) Period 4 (++−−):

$$2\tilde{F} = \omega + 2\tau \ln(1 - e^{-(\omega_{n,m}/\tau)}) + g_0\alpha^2 + \frac{1}{2} g_4\alpha^4 + \frac{g_0^2}{2g_4} + 4(c_1 + 2c_2)\alpha^2 + \frac{1}{2\gamma}\left[6(c_1 + c_2) + g_0 + 3g_4\alpha^2 + \frac{3g_4}{4\gamma} - \omega^2\right] \tag{A9}$$

$$\frac{\partial\tilde{F}}{\partial\alpha} = g_0\alpha + g_4\alpha^3 + \frac{3g_4\alpha}{2\gamma} + 4(c_1 + 2c_2)\alpha = 0 \tag{A10}$$

$$\frac{\partial\tilde{F}}{\partial\omega} = \frac{1}{2}\left\{3(c_1 + c_2) + \frac{1}{2}\left[g_0 + 3g_4\alpha^2 + \frac{3g_4}{2\gamma} - \omega^2\right]\right\}\frac{\partial}{\partial\omega}\left(\frac{1}{\gamma}\right) = 0. \tag{A11}$$

Acknowledgment

Part of this work is supported by EEC stimulation programme ST2J-0032-1-GR.

References

Aubry S 1983 *J. Physique* **44** 147
Axel F and Aubry S 1981 *J. Phys. C: Solid State Phys.* **14** 5433
Bak P 1982 *Rep. Prog. Phys.* **45** 587
Bak P and von Boehm J 1980 *Phys. Rev.* B **21** 5297
Benkert C, Heine H and Simmons E H 1987 *J. Phys. C: Solid State Phys.* **20** 3337
Bilz H, Benedek G and Bussmann-Holder A 1987 *Phys. Rev.* B **35** 4840
Bilz H, Büttner H, Bussmann-Holder A, Kress W and Schrödinger U 1982 *Phys. Rev. Lett.* **48** 264
Büttner H and Heym J 1987 *J. Phys. B: At. Mol. Phys.* **68** 279
Coquet E, Peyrard M and Büttner H 1988 *J. Phys. B: At. Mol. Phys.* **21** 4895
Elliott R J 1961 *Phys. Rev.* **124** 346
Feynman R P 1974 *Statistical Mechanics* (New York: Benjamin)
Feynman R P and Kleinert H 1986 *Phys. Rev.* A **34** 5080
Fischer P, Lebech B, Meier G, Rainford B D and Vogt O 1978 *J. Phys. C: Solid State Phys.* **11** 345
Frosch H and Büttner H 1985 *J. Phys. C: Solid State Phys.* **18** 6303
Giachetti R, Togetti V and Vaia R 1988 *Phys. Rev.* A **37** 2165
Gordon M and Villain J 1985 *J. Phys. C: Solid State Phys.* **18** 3919
Heine V and McConnell J D C 1984 *J. Phys. C: Solid State Phys.* **17** 1199
Janssen T 1986 *Incommensurate Phases in Dielectrics* vol I, ed R Blinc and A P Levanyuk (Amsterdam: North-Holland)
Janssen T and Tjon J A 1982 *Phys. Rev.* B **25** 3767

Jensen M H and Bak P 1983 *Phys. Rev.* B **27** 6853
Kaburagi M and Kanamori J 1974 *Jap. J. Appl. Phys.* suppl 2 381
Katsura S, Ide T and Morita T 1986 *J. Stat. Phys.* **42** 381
Kirkpatrick S, Gellatt C D Jr and Vechi M P 1983 *Science* **220** 671
Selke W 1988 *Phys. Rep.* **170** 213
Toda M 1981 *Theory of Nonlinear Lattices, Springer Series and Solid State Science* vol 20, ed M Cardona, P Fulde and H J Queisser (Berlin: Springer)
Vlastou-Tsinganos G, Flytzanis N and Büttner H 1990 *J. Phys. A: Math. Gen.* **23** 225